Available online at www.sciencedirect.com
ScienceDirect
Journal of Photochemistry and Photobiology A: Chemistry 189 (2007) 387–397
Journal of Photochemistry and Photobiology A:Chemistry
www.elsevier.com/locate/jphotochem

Multi-functional self-cleaning thermochromic films by atmospheric pressure chemical vapour deposition

P. Evans, M.E. Pemble [1], D.W. Sheel, H.M. Yates *

Institute for Materials Research, Salford University, Manchester M5 4WT, UK

Received 19 December 2006; accepted 28 February 2007
Available online 4 March 2007

Abstract

Thin films of titanium dioxide and vanadium dioxide were deposited onto glass using atmospheric pressure chemical vapour deposition (APCVD). The films were investigated as individual layers and as part of multilayer systems to assess their potential to be combined to offer dual functionality, self-cleaning thermochromic films. The multilayer systems were achieved by deposition of vanadium dioxide with subsequent titanium dioxide deposition and vice-versa. XRD revealed that the titanium dioxide existed exclusively in the anatase form and the vanadium oxide either monoclinic VO_2 or mixed vanadium oxides, depending on the position within the multilayer structure. XPS analysis indicated good stoichiometry in the films, and also suggested that the films remained elementally discrete when deposited in the multilayer systems. The multilayered films were active in the destruction of stearic acid layers under UV radiation and showed good thermochromic switching properties.

Furthermore, the titania over-layer imparted a significant degree of enhanced durability to the underlying thermochromic film. This combination of enhanced durability and 'self-cleaning' property, offers interesting potential for wider potential use of this technology.

Keywords: Titania; Vanadium dioxide; Photoactivity; Thermochromic; Chemical vapour deposition

1. Introduction

Added value coatings for glass are of significant commercial and scientific interest, particularly so when grown by atmospheric CVD processes, which have advantages in terms of relatively facile translation into production. The 'self-cleaning' ability of titania arising from its photocatalytic and hydrophilic nature has been the subject of much previous research. Applications have included self-clean glazing products [1], air (and water) purification [2] and antibacterial systems [3].

The thermochromic behaviour [4] of vanadium dioxide, which can give rise to substantial changes in optical IR transmission, arises via the transition from monoclinic to tetragonal rutile structure. Such effects have been explored for solar control glazing applications. Other potential uses of this temperature-induced phenomenon of the semiconductor-to-metal transition for vanadium oxides are lithium-ion batteries and the window in solar cells and gas detectors [5].

Vanadium oxides have been grown by a range of techniques including sol–gel technique [6], vacuum evaporation [7], low pressure [8] as well as atmospheric pressure chemical vapour deposition [9,10].

Known issues with vanadium dioxide include its lack of mechanical robustness and moderate chemical durability. In this paper we explore the use of an over-layer of titania, designed to overcome these limitations. Furthermore, the combination of titania and vanadium oxides gives rise to a multi-functional film demonstrating both the thermochromicity of vanadium dioxide and the high photoactivity of titania, which also imparts a "self-cleaning" surface functionality. We report on the growth and the characterisation of these dual functionality films, all of which were produced in an atmospheric pressure chemical vapour deposition (APCVD) reactor. Through the characterisation we show that the multilayers formed have excellent photoactivity and high optical switching properties. Also, we report on the enhanced chemical durability and regeneration of these films, which when combined with the 'self-cleaning' property, offers interesting potential for wider potential use of this technology.

* Corresponding author. Tel.: +44 161 295 3115; fax: +44 161 295 5111.
E-mail address: H.M.Yates@Salford.ac.uk (H.M. Yates).
[1] Present address: Tyndall National Institute, University College Cork, Lee Maltings, Prospect Row, Cork, Ireland.

1010-6030/$ – see front matter © 2007 Elsevier B.V. All rights reserved.
doi:10.1016/j.jphotochem.2007.02.031

This work represents the first report of both thermochromic and self-clean functional discrete layers within a single multilayered system.

2. Experimental

2.1. Growth

All films were grown on pre-coated (CVD) silica coated barrier glass substrates. The barrier was a (60 nm), amorphous film of SiO_2 designed to prevent diffusion of impurity ions within the float glass (to prevent a reduction in the quality and photoactivity of subsequently deposited film layers). All TiO_2 films were grown using an atmospheric pressure CVD coater described previously [11]. The precursor for titania growth was titanium tetraisopropoxide (7.79×10^{-4} mol min^{-1}) (Aldrich) while the substrate temperature for growth was set to 500 °C. For the vanadium oxides the precursors were vanadium tetrachloride (1.46×10^{-3} mol min^{-1}) (Aldrich) and water (2.3×10^{-6} mol min^{-1}) while the substrate temperature was set to 450 °C. Precursors were transported through the reactor in a nitrogen carrier gas stream.

2.2. Characterisation

Standard techniques of X-ray diffraction (Siemens D5000), uv/visible spectroscopy (Hewlett Packard HP895A) and SEM (Philips XL30) were used to characterise the samples. The morphology of the samples was also assessed by atomic force microscopy (NanoScope IIIa, Digital Inst. Ltd). X-ray photoelectron Spectroscopy, XPS (Kratos AXIS Ultra) with an Al (monochromated) Kα radiation source was used to check the surface composition and stoichiometry of the films. It was necessary to use a charge neutraliser as all the samples were insulating, due mainly to the deposition on glass. This tends to shift the peak positions up to 2 eV so the measurements are referenced to the residual C 1s signal at 285 eV. Curve fitting used CASA XP software using a mixture of Gaussian–Lorentzian functions to deconvolute spectra. Rutherford backscattering was also used to assess the bulk stoichiometry and layer thickness (within the multilayer samples) using an analyzing beam of 2 MeV He^+ with the sample being analysed at normal incidence with a scattering angle of 168° in IBM geometry. Bulk densities for VO_2 of 4.34 g/cm^3 and TiO_2 of 4.23 g/cm^3 were used for the modelling.

The comparative chemical resistance of the samples was tested by soaking the samples in 2 M sodium hydroxide solution and using an optical microscope to assess the changes.

Photocatalytic behaviour was measured under UV radiation (365 nm) and visible radiation by use of a high intensity lamp (300 W) with a 400 nm cut-off filter. The degradation of stearic acid was followed by FTIR (Bruker, Vector 22). Stearic acid (100 μl of 10 mmol in methanol) was spun-coated onto the sample. After drying in an oven at 55 °C the sample was exposed to UV light with an intensity of 3 mW cm^{-2}. The activity of the film was defined in cm^{-1} min^{-1}, which indicated the rate of reduction in selected stearic acid peaks in the IR region. The technique used [12] was developed from work described previously [13–15].

The optical properties of the films were measured on a nkd8000 spectrophotometer (Aquila Instruments Ltd) with an incorporated heating stage. Samples were heated from room temperature to 75 °C in 5 °C intervals, in order to observe and assess the thermochromic transition. A wavelength range from 800 to 1700 nm was used with s-polarised incident light at an angle of 30°.

3. Results and discussion

Using atmospheric pressure CVD, multilayers of TiO_2 with an underlayer of VO_2 (TiO_2 on VO_2 on SiO_2-coated glass) and the inverse (VO_2 on TiO_2 on SiO_2-coated glass) were grown. As references, single layers of TiO_2 and VO_2 on glass were also grown under identical conditions, comparable in thickness to the multilayer composites.

3.1. Visual

All films were transparent with less than 2% haze. In the case of the reference TiO_2, the haze was less than 0.5%. Those films containing the vanadium oxides had a greenish tinge, while the reference titania sample was brown due to interference colouration.

3.2. X-ray diffraction

The reference samples of titanium dioxide and vanadium dioxide showed polycrystalline peaks for anatase (JCPDS 21 1272) and monoclinic vanadium dioxide (JCPDS 44 0253), respectively (Fig. 1). X-ray diffraction for the vanadium oxide also showed small signals at 25.3° and 14.6°, which have been assigned to tetragonal V_2O_5 (JCPDS 45 1074). Assignment of all the XRD features can be complex since anatase, rutile and the many forms of vanadium oxides have a number of peaks in similar positions.

Growth of TiO_2 on a VO_2 layer (grown as the reference) established that the TiO_2 was anatase, with monoclinic VO_2 as the underlayer. This suggests that no change occurs within the

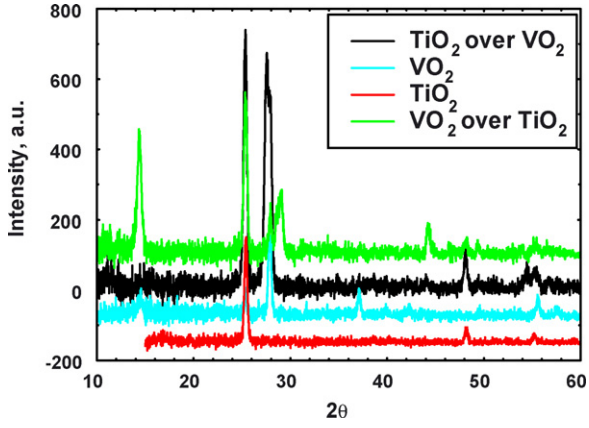

Fig. 1. XRD of multilayer samples and corresponding references.

VO_2 on heating to 500 °C during the deposition of TiO_2. This is not very surprising as the temperature is not much higher than that used to grow the VO_2. However, it is interesting that at this temperature the VO_2 would be expected to be in a tetragonal rutile form and perhaps have a structure-directing influence on the TiO_2 formation with the production of rutile. This does not occur and only anatase is deposited, as established by XRD. This is perhaps still more surprising since Carotta et al. have shown that although for a quite different growth process (sol–gel), that addition of V ions aids the transformation of anatase to rutile on annealing [16].

XRD analysis of the multilayer of TiO_2 capped with an over-layer of VO_2 confirmed the TiO_2 was anatase, with the over-layer containing mainly V_2O_5 (JCPDS 45 1074) although the XRD data contained some contributions from monoclinic VO_2 (27.9° and 55°) and also possibly some orthorhombic V_2O_5 (JCPDS 41 1426) at 44.2° and 49.5°.

The presence of a mixture of vanadium oxides meant that an unambiguous assignment of the XRD data was difficult due to the lack of sufficient numbers of peaks required for accurate indexing.

Since for the two layer structures essentially identical growth conditions were employed, the differences in the nature of the VO_2 films formed in each case can be attributed to the influence of the morphology of the underlying layer—in one case amorphous SiO_2 and in the other TiO_2 in the anatase form. In this respect, it is noteworthy that there is a 3.6% lattice mismatch between TiO_2 and VO_2 and thus growth of VO_2 on TiO_2 may lead to a highly strained system. This may account for the mixture of vanadium oxides found for these samples.

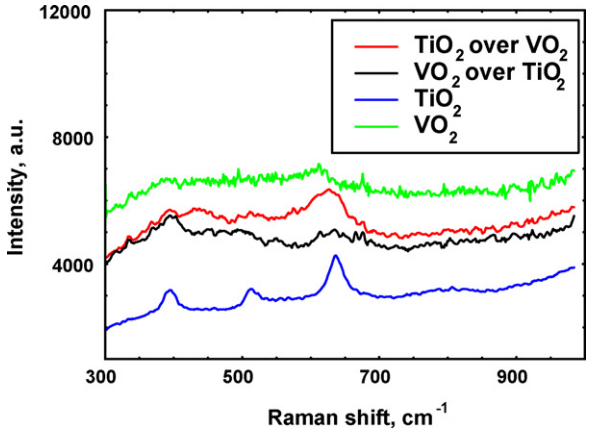

Fig. 2. Raman of the multilayer samples and their references.

3.3. Raman spectroscopy

Raman excitation at 514 nm was used to confirm the type of TiO_2 present. To study the vanadium oxides longer wavelength

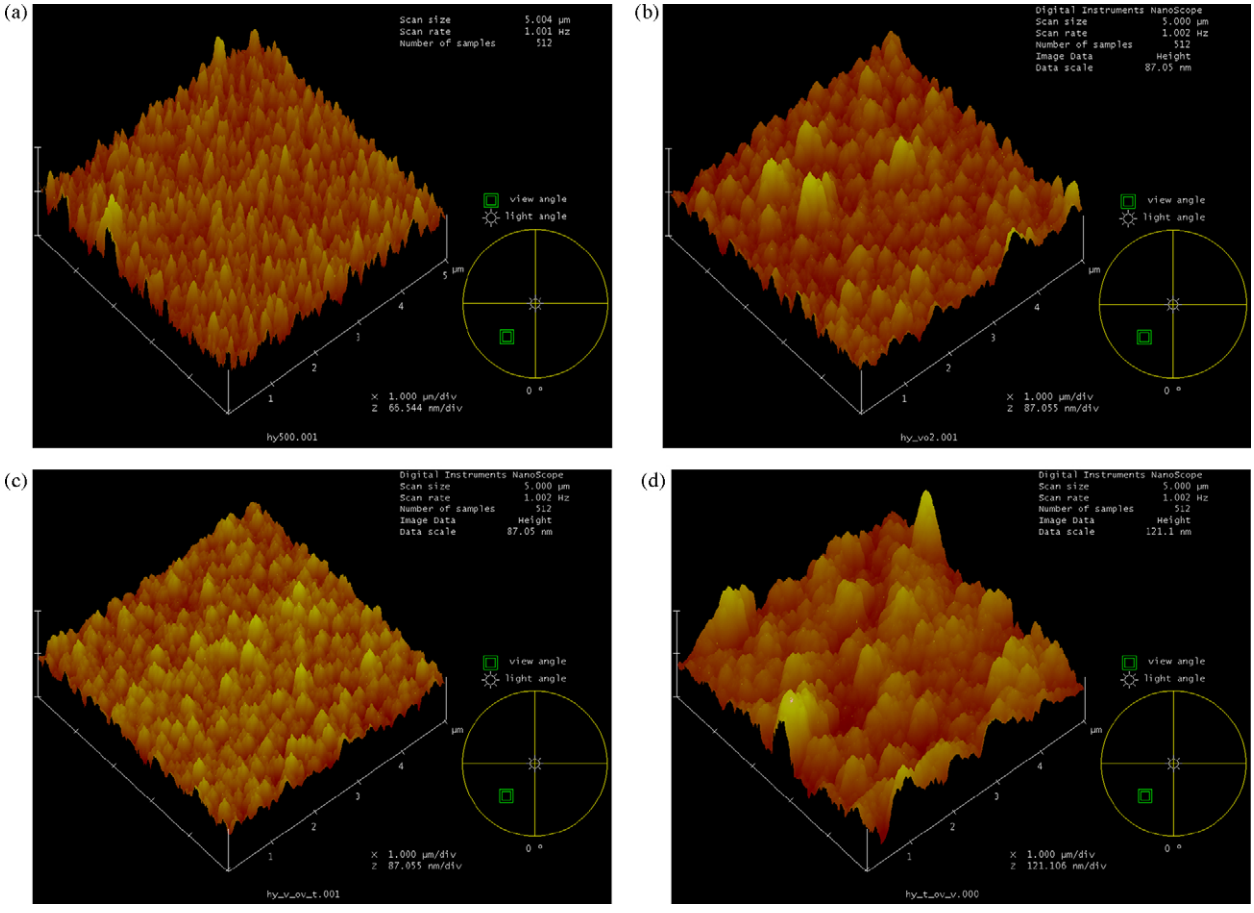

Fig. 3. AFM images, (a) TiO_2, (b) VO_2, (c) VO_2 over TiO_2 and (d) TiO_2 over VO_2.

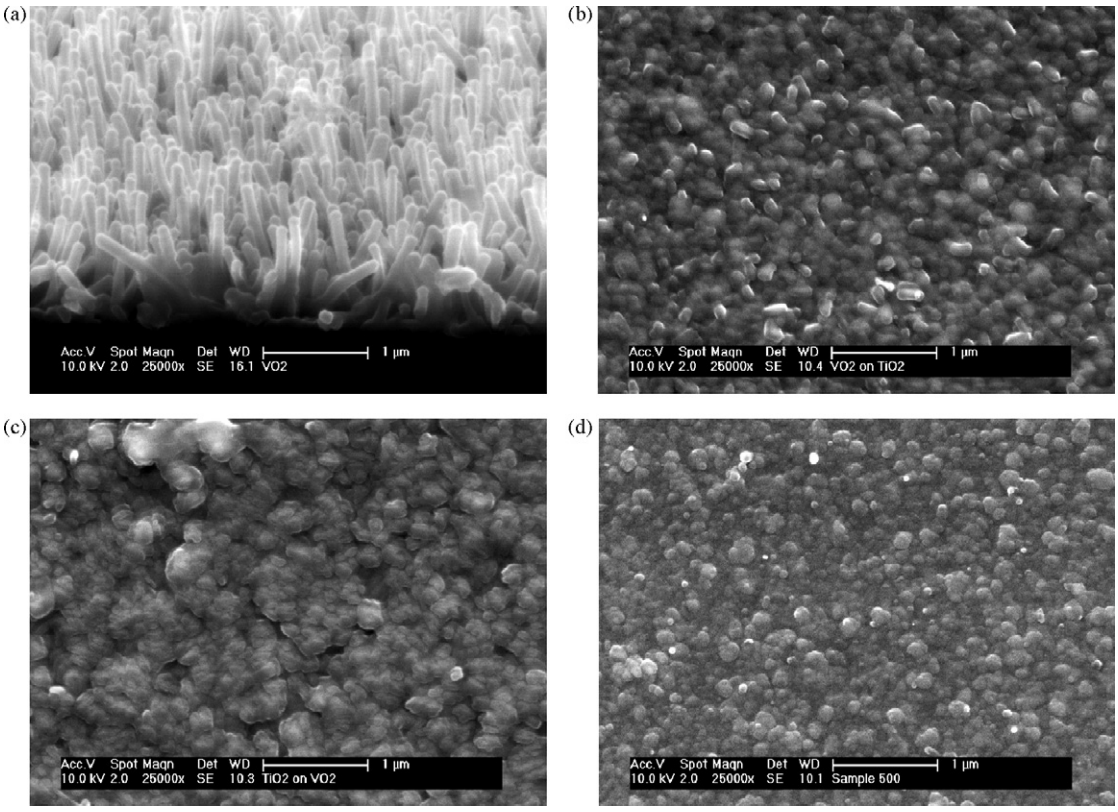

Fig. 4. SEM images of (a) VO_2, (b) VO_2 over TiO_2, (c) TiO_2 over VO_2 and (d) TiO_2.

excitation would be necessary in order to avoid direct absorption of the laser line via the coloured vanadium oxide films. Unfortunately longer wavelength excitation was not available. Raman confirmed that the main form of TiO_2 was anatase (397, 515 and 636 cm^{-1}), although for the sample of TiO_2 grown on VO_2 Fig. 2 reveals that there may be a very small amount of rutile (not detected by XRD), giving rise to the broad peak at 438 cm^{-1} and the possible shoulder at 604 cm^{-1}.

3.4. Morphology

AFM of the various samples (Fig. 3) established that there was comparatively little difference in morphology and roughness of the reference VO_2 and the multilayer of VO_2 over TiO_2, at both the 5 μm × 5 μm and the 1 μm × 1 μm scale. That of the VO_2 reference having slightly less uniformity over the scale studied. In contrast, this was not the case for the reference TiO_2 sample and the multilayer of TiO_2 over VO_2. The morphology of the TiO_2 reference sample was similar in uniformity and level of roughness to the previous samples, while that of the multilayer (with a TiO_2 over-layer) was much less uniform. In Fig. 3(c and d) a comparison of the multilayers is shown. As can be seen the TiO_2 over VO_2 sample is less uniform in overall structure with a Ra value (21.2 nm, taken from the 5 × 5 plot) at least double that of the VO_2 (10.3 nm), TiO_2 (7.95 nm) or VO_2 on TiO_2 (7.8 nm) samples.

The increased roughness of the multilayer of VO_2 with an over-layer of TiO_2, Fig. 3(d), possibly relates to increased lattice strain as previously mentioned. However, when VO_2 is grown on TiO_2, Fig. 3(c), the VO_2 coating appears to adopt the texture and contours of the underlying TiO_2 film. Given that the lattice strain argument should apply in both cases, this result suggests that the growth of the VO_2 is more strongly influenced by the morphology of the TiO_2 under layer, to the extent that the under layer acts as a template for growth, which locks in a particular feature size at the expense of the formation of monoclinic VO_2. This argument would be consistent with the XRD data for these samples, which showed that they contained a mixture of vanadium oxides.

SEM of the samples gave a more general view of the morphology, confirming the uniformity of the surface over a wider area. As can be seen in Fig. 4(a) the reference VO_2 sample showed a rod like structure, generally aligned perpendicular to the substrate. These rods were about 108 nm in diameter, with some reaching 800 nm in length. Similar VO_2 rod like structures were seen by Manning and Parkin [17] and also by Qureshi et al. [18] in composite TiO_2–VO_2 films, although in the latter paper their rods were thicker, relating probably to the higher growth temperature used.

However, for growth of VO_2 on top of TiO_2, the surface became more compact, with uniform granular particle morphology (Fig. 4(b)). This structure is similar to that seen by both Sahana et al. [19] and Vernardou et al. [9] for VO_2 grown using vanadyl acetylacetonate rather than vanadium tetrachloride. Growth of TiO_2 over VO_2 (Fig. 4(c)) led to a structure characteristic of anatase growth directly on glass (Fig. 4(d)).

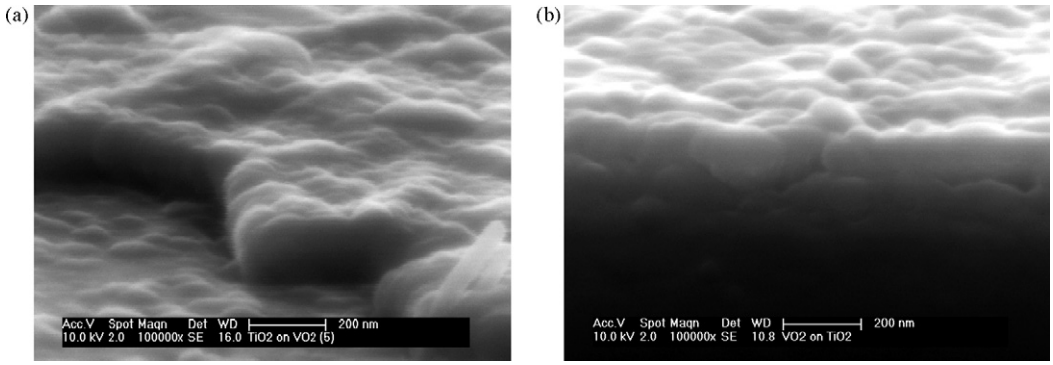

Fig. 5. SEM cross-sectional images of (a) TiO_2 over VO_2 and (b) VO_2 over TiO_2.

Comparison of both multilayers suggested that that of the TiO_2 over VO_2 sample was slightly rougher, although finer detail of the AFM was required to confirm this.

The individual layer thicknesses were assessed using cross-sections (Fig. 5), but it was difficult, particularly for TiO_2 over VO_2, to distinguish the individual components within the multilayers. The smoother transition from VO_2 to TiO_2 (than the inverse growth) suggested that the TiO_2 locked into the underlying structure, taking up the lattice mismatch by internal strain rather than reduction by dislocations and structure changes (as confirmed by XRD), which occurred for TiO_2 over VO_2.

The deposition thickness, established by SEM, was 158 nm for TiO_2 over VO_2 and 198 nm for VO_2 over TiO_2. That for VO_2 over TiO_2 could be split into 112 nm for VO_2 and 86 nm for TiO_2. The samples were grown under identical conditions so the difference in thickness was probably due to growth rate changes caused by the different underlying layers.

3.5. Rutherford backscattering spectroscopy

To identify the thickness of the individual composite of the TiO_2 over VO_2 sample and confirm the bulk compositions and other thickness values it was necessary to use RBS. By fitting the experimental data it is possible to obtain the bulk stoichiometry, although not the oxidation states. By further modelling of the data either the thickness or density can be obtained, as these two parameters are dependent on each other. Fig. 6 shows examples of the RBS measurements, with the points being the experimental data and the line the modelled fit. Sharp cut-offs (beginning and ends) relating to Ti and V can be seen, as they are distinct layers within the sample. However, the O is seen as a rising edge as it is present in both layers and the substrate. Also present are signals relating to the SiO_2 glass substrate and its impurities (Na and Ca). There is no sign of any carbon contamination in the bulk sample.

In Fig. 6(a) for VO_2 over TiO_2 the RBS shows 2 distinct peaks for V and Ti, while in Fig. 6(b) for TiO_2 over VO_2 only one peak for Ti and V is seen. The element with the greater mass will be at a higher channel number, so for a material with both Ti and V on the surface V would start at 295 and Ti at 287. However, for a multilayer the position of the lower element becomes shifted to lower channel numbers, which would lead to a separation of the signals for VO_2 over TiO_2 (Ti shifting to lower channel numbers) and an amalgamation of the signals for TiO_2 over VO_2.

For all three samples analysed (VO_2, TiO_2 over VO_2 and VO_2 over TiO_2) they were all confirmed to be stoichiometric V_1O_2 and Ti_1O_2. This is in agreement with the X-ray diffraction results for VO_2 and TiO_2 over VO_2. However, the X-ray diffraction result for the vanadium oxide sample over TiO_2 concludes that the upper layer consists of mainly V_2O_5 with a little VO_2. Attempts to fit the RBS data to obtain an increase in the amount of oxygen were not successful. To explain this apparent contradiction it is necessary to consider the possibility that the V_2O_5 is mainly a surface layer with VO_2 underneath. In this case glancing angle X-ray diffraction would give a greater weighting

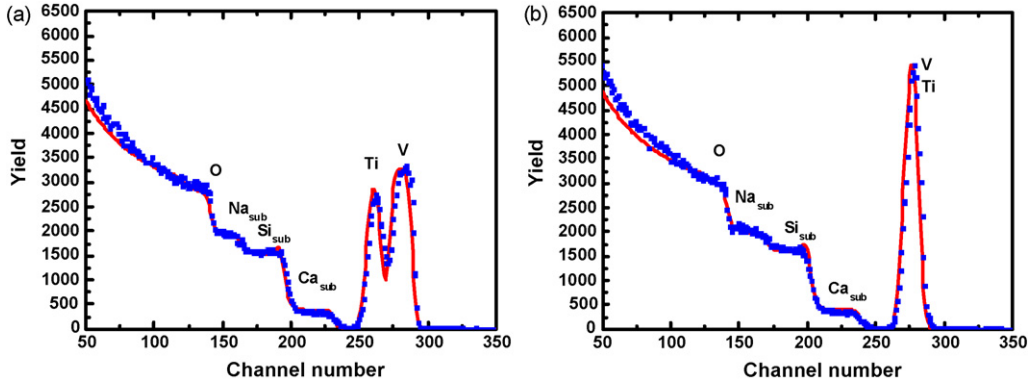

Fig. 6. RBS measurements for (a) VO_2 over TiO_2 and (b) TiO_2 over VO_2.

to the surface. A secondary confirmation of the presence of a reasonable amount of VO_2 is shown later in the thermochromic measurements. If no or negligible VO_2 was present there would not have been a well defined thermochromic change round 55 °C.

The component layers for VO_2 over TiO_2 were calculated to be 100 nm and 70 nm, respectively. These values are in agreement with those obtained from the SEM for VO_2 and TiO_2 layers of 112 ± 11 nm and 86 ± 12 nm, respectively. The TiO_2 over VO_2 sample gave 70 nm for VO_2 and 55 nm for the TiO_2 layer. The total sample thickness of 125 nm is lower than that from the SEM of 158 ± 17 nm. The VO_2 sample (grown under identical conditions to that in the multilayers) also gave a thickness of 70 nm. This thickness discrepancy relates to the use of the bulk densities of the components in the modelling. The density is inversely proportional to the layer thickness. It is very likely that the density of the VO_2 under the TiO_2 is lower than the VO_2 deposited on top of TiO_2 and that of the bulk value when considering that it will be in the same porous form as the reference VO_2 sample, as seen in the SEM morphologies.

3.6. X-ray photoelectron spectroscopy

No samples showed any sign of any impurities, except for carbon, which was to be expected. Both multilayer samples established that only the top layer could be detected by XPS, confirming the formation of coherent films with no pin-holes or diffusion to the surface of other chemical species. Confirmation of this can be seen in Fig. 7 where the high resolution scans for Ti 2p and V 2p are show for both samples.

For the TiO_2 over VO_2 sample, the Ti 2p spectrum showed the expected $2p_{1/2}$ and $2p_{3/2}$ features at 465.05 and 459.28 eV, respectively, which relate to Ti^{4+} attached to O^{2-} [20], with a splitting of 5.77 eV. There was no shift in position from that of the reference TiO_2 sample. Again the width of the peaks at 0.80 eV is in line with that seen for the reference (0.86 eV) and is indicative of TiO_2 with low structural disorder [21]. High resolution O1s spectra confirm the presence of TiO_2 (530.05 eV), along with a low intensity signal at 531.82 eV relating to absorbed water [22].

The V 2p spectrum, for the VO_2 over TiO_2 sample, is similar to that of the reference VO_2 sample in both position ($2p_{3/2}$ at approximately 516.4 eV, with a splitting of 7.68 eV) and width. This is the position for a vanadium oxide (515.5–517.5 eV) [23], but accurate assignment of this feature is complicated by spectral asymmetry broadening towards higher B.E., which could be misinterpreted as a shoulder for the next oxidation state. Due to this it is more usual to discuss the average oxidation state via the positions of the raw data relative to the O 1s signal [24].

$$V_{ox} = 13.82 - 0.68\,(\mathrm{O\ 1s} - \mathrm{V\ 2p_{3/2}})$$

These calculations led to identical average oxidation states for the reference VO_2 and that of the multilayer of 4.7. Looking closely at the V 2p spectrum it is possible to resolve this into 2 species of average oxidation state 4.4 and 5.2. The multilayer and VO_2 reference samples being approximately 49 and 35% average oxidation state 4.4, respectively. However, it is important to bear in mind that these figures do not necessarily reflect the structure of the bulk or as grown sample. In comparison the bulk stoichiometry was confirmed by RBS, which also agrees with the XRD result for TiO_2 over VO_2.

Another issue with XPS of vanadium is the tendency of the lower oxidation states to oxidise to V^{5+} (most stable state V_2O_5) when exposed to ambient conditions. As XPS is a surface sensitive technique sampling a depth of approximately 5 nm it is this state that is most readily detected. In theory etching the top surface via an Ar^+ ion beam should help, but in practice this leads to the reduction of the V species [25]. All this makes it difficult to extract full details of exact chemical species present.

3.7. UV/visible spectroscopy

The absorbance of the thermally grown TiO_2 reference gave a sharp peak at 318 nm, while that of the VO_2 had a much broader

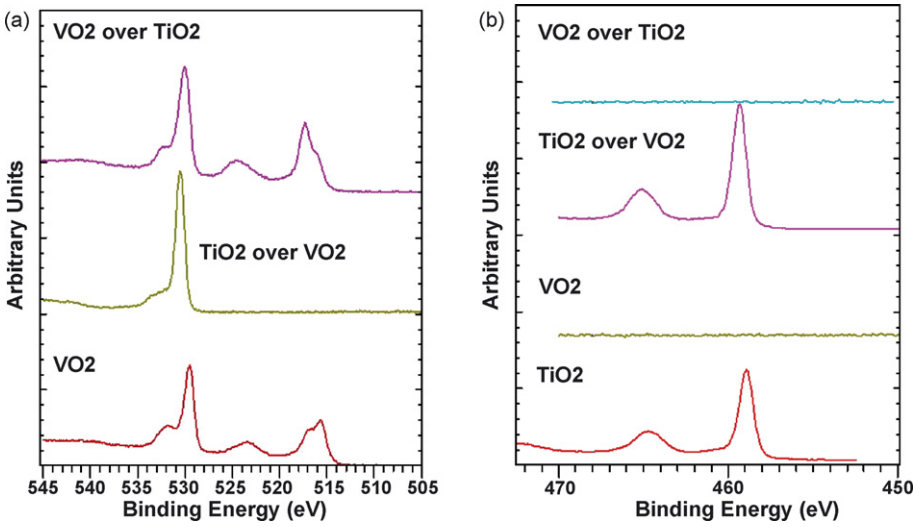

Fig. 7. XPS of (a) O 1s and V 2p and (b) Ti 2p.

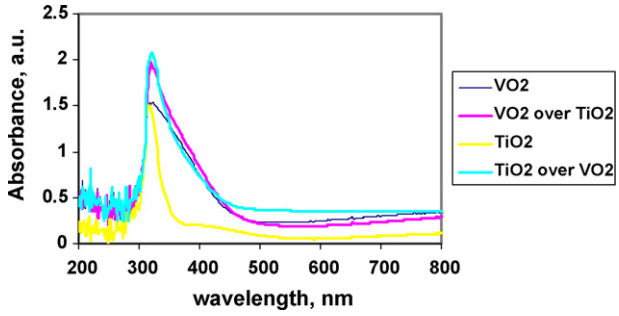

Fig. 8. UV/visible absorbance spectra.

signal to lower energy, Fig. 8. This was to be expected due to the colouration of the VO_2.

The appearance of a peak, rather than an edge, is due to removal of the background from the glass substrate (so only the effects of the deposited film were seen) and the uncorrected spectral response of the spectrometer. As can be seen in Fig. 8, the multilayer samples gave basically an amalgamation of these signals, although with a small shift of the TiO_2 band edge to 322 nm.

3.8. Contact angle

Results shown, in Table 1, are the average of 5 angle measurements for before and after 60 min of 365 nm, 3 mW cm^{-2} UV radiation. These are for samples at room temperature. All samples showed a reduction in the contact angle after UV radiation, showing an increased hydrophilicity.

That of the VO_2 with an over-layer of TiO_2 showed the greatest overall change, along with the lowest angle after radiation. The after radiation value is comparable with the reference TiO_2 sample, although the pre-radiation value is higher showing a slightly increased hydrophobic nature. Overall there was no adverse change in the hydrophilicity by growth on VO_2 rather than directly on glass. Although the two samples of VO_2 (direct on glass or via a layer of TiO_2) have very different morphologies (as seen by the SEM) the actual changes and values of the contact angle are very similar.

3.9. Thermochromic properties

To assess the thermochromic behaviour of the samples the reflection and transmission were measured at a range of temperatures. Care was taken (using a hand held temperature probe) to assure that the sample surface had reached the required temperature and not just the heating stage. A 5 °C difference in

Table 1
Contact angle results

Sample	Before UV radiation (°)	After UV radiation (°)
TiO_2 over VO_2	63.70 ± 2.85	18.45 ± 2.23
VO_2 over TiO_2	54.30 ± 0.77	40.91 ± 7.98
VO_2	54.50 ± 2.54	32.30 ± 2.50
TiO_2	56.51 ± 1.46	18.00 ± 0.88

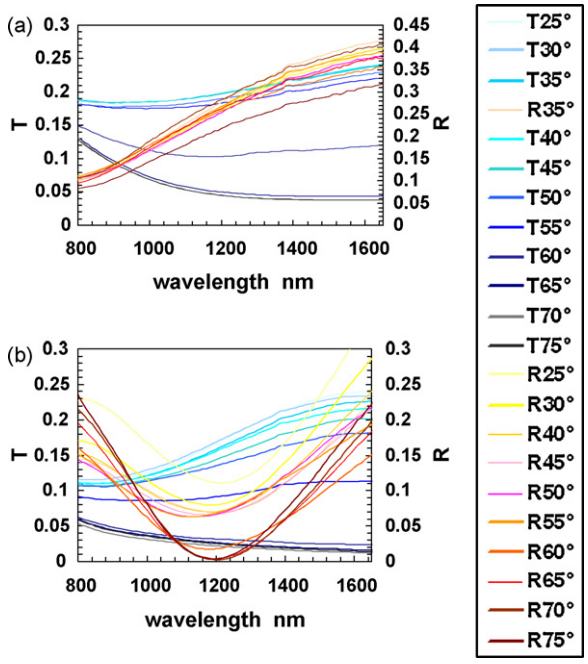

Fig. 9. Reflection and transmission spectra changes with temperature (a) VO_2 and (b) TiO_2 over VO_2.

stage temperature and sample temperature was observed. All measurements shown give the temperature of the sample.

The reflection and transmission spectra shown in Fig. 9(a) show a relatively simple structure for the reference VO_2. The transmission spectra have a blue tone and the reflection have a red or yellow tone legend.

A clear change, particularly in the transmission curve can be seen to be occurring from 55 to 65 °C. These spectra become more complex as TiO_2 is added to the structure. For example Fig. 9(b) shows the spectra for TiO_2 over VO_2. There is now more structure particularly to the reflectance curves. Again the transition between the monoclinic and tetragonal VO_2 structure reflected in the optical change can be seen between 50 and 60 °C.

To more accurately pin-point the temperature at which the change occurs, values of reflectance and transmission were extracted at 1500 nm and plotted against temperature. Although both the reflection and transmission changes can be seen (Fig. 10), the change in the transmission is particularly apparent.

The sample of TiO_2 over VO_2 had a lower temperature switching point than that of the VO_2 reference, which was marginally better than that of the VO_2 over TiO_2 structure. For a more quantitative analysis of the thermochromic effect, temperatures were chosen at which complete change would have occurred, i.e. 25 and 65 °C. From these values the percentage change in available light was calculated as shown below. The results are shown in Table 2.

$$\frac{T_{25} - T_{65}}{T_{25}} \times 100 = \%\text{change};$$

$$\frac{R_{25} - R_{65}}{R_{25}} \times 100 = \%\text{change}$$

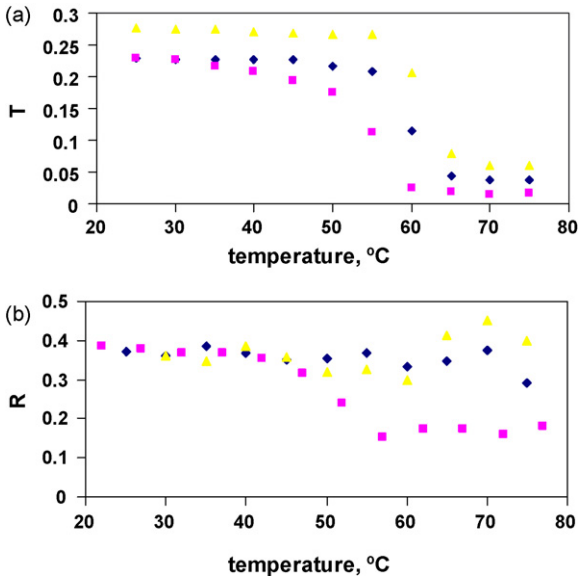

Fig. 10. Optical data at 1500 nm. (a) Transmission measurements VO_2 ♦, TiO_2 over VO_2 ■, VO_2 over TiO_2 ▲. (b) Reflection measurements.

For all three samples, there was a decisive reduction in transmission over the VO_2 transition temperature. However, the reflectance change was not as clearly marked, being over a smaller range of values, with a comparatively higher degree of scatter.

A greater change in reflectance was shown for the multilayer samples than that of the individual VO_2 sample. Interestingly, the VO_2 sample with an over-layer of TiO_2 showed a decrease in reflectance at the transition temperature, while that of the TiO_2 sample capped with VO_2 showed an increase. This observation may be understood by considering the interaction of the relative refractive indices in the multilayers, and especially the change in refractive index of the VO_2 upon transition from the monoclinic to the tetragonal crystal system (the precise value for particularly VO_2 depending on growth conditions. VO_2 monoclinic; $n = 2.8$–3.20 [26,27], VO_2 tetragonal; $n = 1.1$–1.6 [26], TiO_2 anatase; $n = 2.5$, air; $n = 1$). The basic concept of relevance is that used in simple colour suppression layers, where via a judicial matching of refractive indices present in multilayer systems interference effects can be used to tailor the appearance of a film, over selected wavelength regions [28]. When a wave is reflected from the surface of a material of higher refractive index it ideally undergoes a 180° phase change, but when the material has a lower refractive index there is no phase change. In the case of the TiO_2 over monoclinic VO_2 there is an increase in refractive index at each subsequent surface (air < TiO_2, TiO_2 < VO_2), hence the light reflected at the air/TiO_2 interface undergoes a 180° phase reversal, and the light reflected on the TiO_2/monoclinic VO_2 interface also undergoes a 180° phase, these waves therefore emerge constructively. When the sample is heated above the transition temperature, the VO_2 becomes tetragonal and has a lower refractive index than that of the TiO_2, the light involved in the second reflection (i.e. on the VO_2 surface) does not undergo a phase change, therefore the light reflected from the two interfaces emerges destructively. This is in agreement with our observations, the reflectance of the TiO_2 over VO_2 sample decreased above the transition temperature.

In the case of VO_2 over TiO_2, below the transition temperature (i.e. in the monoclinic form), there is a phase change at the air/VO_2 interface (air < VO_2 monoclinic) but no phase change at the VO_2/TiO_2 interface (VO_2 monoclinic > TiO_2), these waves therefore emerge destructively. Above the transition temperature the tetragonal VO_2 has a refractive index lower than TiO_2, therefore a phase change occurs at both interfaces, and these waves emerge constructively. This is also in agreement with our observations, the reflectance of the VO_2 over the TiO_2 sample increased above the transition temperature.

The phase shift upon reflection depends also on the relationship between wavelength and layer thickness. In the specific case where the layer thickness = $\lambda/(4n)$ then complete destructive interference will arise. However, this is a very specific case and for this reason does not generally apply. Thus, overall, at any given wavelength there will be a contribution towards loss of intensity as a result of interference, but by far the most significant effects will arise from a consideration of relative refractive indices.

Within the literature no exact comparison could be found in terms of switching temperatures, due to the fact that the multilayer systems described here have not been made previously. All samples containing VO_2 (multilayers and reference), switched between 50 and 60 °C—temperatures which are comparable to those reported previously with values ranging from 70 °C [29], through 68 °C [19,30,31] to 53 °C [18]. The higher switching temperatures relate to VO_2 only, while the lower values relate to a film containing a mixture of mainly VO_2 doped with some TiO_2 [18]. In this work, the reduction in switching temperature was considered to be due to the effects of strain induced by the TiO_2 within the VO_2. The presence of strain within the VO_2 layer would help explain the reduced switching temperature for the TiO_2 over VO_2 sample studied here as compared to the VO_2 reference. However, little difference was seen in the VO_2 over TiO_2 sample despite the presumed presence of strain. From other studies on the effect of strain on the switching temperature the orientation of the underlying layer is of importance, leading to increases or decreases in transition temperature [32]. Therefore, the change produced is a product of the various strains the growing layer is under. In our case, we noted earlier that for the VO_2 over TiO_2 sample, the morphology of the VO_2 film was essentially that of the underlying TiO_2 film, which appears to act as a template for growth. Thus, it is possible that morphology, possibly grain size, is the dominant factor here, rather than strain itself.

Table 2
Percentage transmission and reflectance changes

Sample	Transmission change (%)	Reflectance change (%)
VO_2	81	6
TiO_2 over VO_2	92	55
VO_2 over TiO_2	71	−55

Table 3
Data for solar calculations above and below the transition temperature for VO_2 containing samples

Sample	%Transmittance	
	25 °C	65 °C
TiO_2 over VO_2	12.9	4.9
VO_2	18.8	10.9
VO_2 over TiO_2	22.9	14.6

From this data solar transmittance can be calculated according to a standard solar energy distribution curve defined by the ASTM which represents average solar irradiation at sea level in the middle of the northern hemisphere. This assumes a tilt of 37°, which is the average angle of the sun's rays impinging off a vertical surface (in the Northern hemisphere). This was calculated for the samples both above (65 °C) and below (25 °C) the VO_2 transition temperature. The data is shown in Table 3.

It was shown that the percentage transmittance (in IR) fell, as would be expected, after the VO_2 transition to the tetragonal rutile form. That for TiO_2 over VO_2 showed the greatest change and the lowest IR (i.e. heat) transmittance after the VO_2 transition temperature. For a glazing application this reduced IR transmittance after the transition temperature would be an advantage. Indeed, for some potential application areas (e.g. automotive roof-lights) low transmission levels are desired.

3.10. Photocatalytic behaviour

This was determined by the decomposition of stearic acid under both UV and visible light. It can be seen in Fig. 11 that as expected the TiO_2 reference is highly photoactive, while the VO_2 reference is not ($0.0004\,cm^{-1}\,min^{-1}$). From tests using standard float glass a gradient of $\leq 10^{-4}\,cm^{-1}\,min^{-1}$ is assumed to represent an inactive sample. The sample of TiO_2 over VO_2 is also photoactive ($0.0057\,cm^{-1}\,min^{-1}$) comparing favourably to the activity of the reference ($0.0046\,cm^{-1}\,min^{-1}$).

No literature data was found for multilayers comparable to those described here, but for sol–gel mixtures of TiO_2 with vanadium in different oxidation states (V^{5+} [33,34], V^{4+} [35,36])

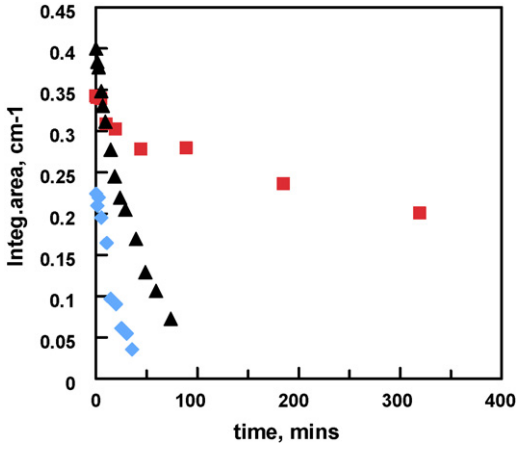

Fig. 11. UV photoactivity for TiO_2 on VO_2 ♦, VO_2 ■ and TiO_2 ▲.

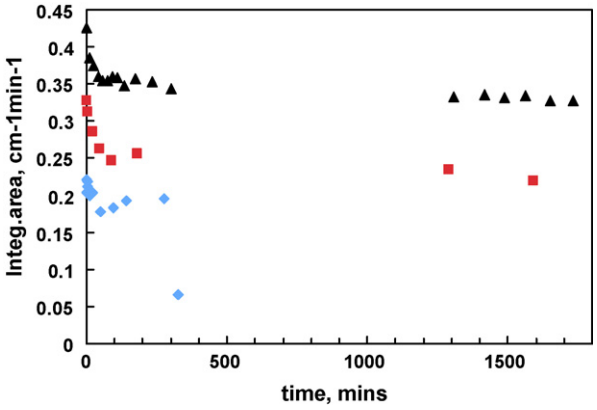

Fig. 12. Visible activity of TiO_2 on VO_2 ♦ and references VO_2 ■ and TiO_2 ▲.

addition of V ions was considered to improve the photoactivity of the materials. However, too great a doping level of V in TiO_2 was expected to reduce photoactivity activity [37]. Only one research group has used CVD to produce mixed films of TiO_2 and VO_2, rather than the discrete multilayers described here. The authors [38] suggested that the VO_2 films exhibited proportional photoactivity to the titania present in the layer, although no values were given.

From Fig. 12 it can be seen that no visible activity was seen (or expected) for VO_2 or TiO_2 ($10^{-5}\,cm^{-1}\,min^{-1}$). In the literature there are some claims for visible activity of V-doped TiO_2. Earlier work [39] reported that doping TiO_2 with V shifted the bandgap toward the visible part of the spectrum and in some cases reported photoactivity in the visible [40,41]. However, in spite of the band edge shift towards longer wavelength for our multilayered samples the measured rate of reaction was $10^{-4}\,cm^{-1}\,min^{-1}$ and thus no visible activity was observed.

This lack of visible activity could be due to the lack of interaction between layers, as established by XPS with no detectable doping caused by ion migration. However, previous reports in the literature for doped TiO_2–V gave a very mixed opinion as to the existence or otherwise of true visible light photoactivity while the lack of visible activity and reduced UV activity observed in our experiments was in good agreement with the findings of many other groups [42,43]. Also, we note that in some cases where visible light induced photoactivity had been claimed, the experimental methodologies employed have been questionable- for example via the failure to adequately filter out uv light during the measurements [41].

3.11. Durability

All films adhered strongly to the substrate (as determined by the adhesive-tape peel test). Bulk vanadium oxides are amphoteric, dissolving in both acids and alkalis [44]. So to assess the degree to which the TiO_2 layer could act as a protective (as well as self-cleaning) coating towards the underlying VO_2, samples of VO_2 and TiO_2 over-coated VO_2 were placed in a 2 M NaOH aqueous solution for 4 h. The relatively aggressive conditions (compared to potential "in use" exposure) were specifically chosen to show the dramatic protective effect provided by the

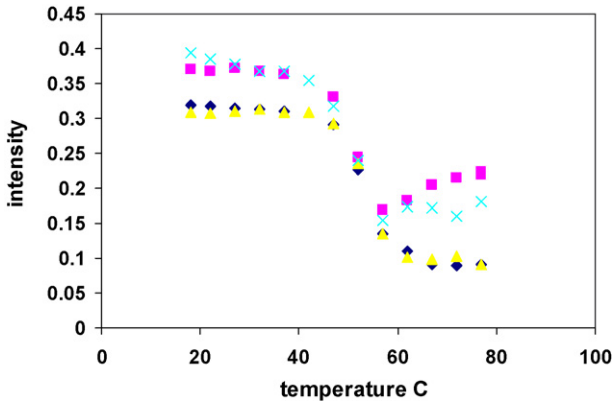

Fig. 13. Spectrophotometry data for comparison of TiO_2 over VO_2 before and after NaOH etch. Reflection before x and after ■, transmission before ▲ and after ♦.

TiO_2 layer. The edges of the samples were masked using PVC adhesive-tape to prevent 'peeling' of the TiO_2 over-layer via dissolution of the VO_2 underlayer as a result of contact with the alkali at the exposed edges.

After 4 h the VO_2 had completely dissolved in the exposed area, this was expected and was in line with previously reported work [25]. Upon removal of the tape around the edges, the coating remained intact and clearly visible, showing good adhesion to the substrate. The exposed TiO_2 surface remained unchanged, showing no visible signs of degradation or dissolution to eye or optical microscope. Upon removal of the PVC tape the coating remained intact, indicating good inter-layer and substrate adhesion. Subsequent XRD of the sample showed the structure of both the TiO_2 and the VO_2 were unchanged, and XPS analysis only detected peaks corresponding to TiO_2 with no vanadium detected, confirming that the surface was still intact with no pin-holes.

The sample was re-tested for its photocatalytic activity, the sample remained highly photoactive ($0.0040\,cm^{-1}\,min^{-1}$), showing only a small decrease compared to its photoactivity ($0.0057\,cm^{-1}\,min^{-1}$) before the durability test. Such a small decrease in photoactivity after exposure to such aggressive testing again highlights the resilience of TiO_2 as a protective layer.

As a final test to confirm the durability of this sample the thermochromic behaviour of the VO_2 underlayer was again tested (after the NaOH etch). There was no change in the switching temperature or in the absolute transmission and reflection of the sample, beyond that of instrumental and experimental error variation, as can be seen in Fig. 13.

4. Conclusions

APCVD has been used to deposit thin films of VO_2, TiO_2 and their combinations. All materials were shown to be polycrystalline, consisting of anatase for the TiO_2 layers, and either monoclinic VO_2 or mixed vanadium oxides. All samples containing vanadium oxide species showed thermochromic properties with the lowest switching temperature recorded being 55 °C for a sample of VO_2 with an over-layer of TiO_2. This temperature was lower than that of the reference VO_2 sample due to the strain within the system. Photocatalytic behaviour, in the UV, with the degradation of stearic acid for TiO_2 over VO_2 was comparable to that of the reference TiO_2 sample.

With a multilayer of TiO_2 over VO_2 we have produced layers, which show the combined functionality of photoactivity with that of thermochromicity. The resulting dual layer system displays enhanced resistance to chemical attack as compared to the reference VO_2 film alone.

This work has demonstrated for the first time, the efficacy of the APCVD approach for the fabrication of films, which show dual functionality in the form of protection/self-cleaning and thermochromicity. It is anticipated that this approach could offer commercial potential in the production of glazing units designed to reduce building and vehicle energy costs while requiring minimal routine maintenance. In particular, the enhanced durability offers potential for monolithic (i.e. single pane) glazing which can have major cost benefits and is an attractive option in certain climates. As such these dual layer systems represent a potentially major step forward in the development of smart glazing materials.

Acknowledgements

This work is financed by the EC through GRD1-2001-40791, PHOTOCOAT project. We would also like to thank Aquila Instruments Ltd for the spectrophotrometry temperature measurements, M. Faulkner from University of Manchester Materials Science Centre for the SEM images and R. Valizadeh, Manchester Metropolitan University for the RBS data.

References

[1] http://www.pilkington.com http://www.saint-gobain.com.
[2] M.A. Fox, M.T. Dulay, Chem. Rev. 93 (1993) 341–357.
[3] Y. Kikuchi, K. Sunada, T. Iyoda, K. Hashimoto, A. Fujishima, J. Photochem. Photobiol. A 106 (1997) 51–56.
[4] C.H. Griffiths, H.K. Eastwood, J. Appl. Phys. 45 (1974) 2201–2206.
[5] J.F. De Natale, P.J. Hood, A.B. Harker, J. Appl. Phys. 66 (1989) 5844–5850.
[6] V. Vivier, J. Farcy, J.P. Pereira-Ramos, Electochim. Acta 44 (1998) 831–839.
[7] Z.S. Guan, J.N. Yao, Y.A. Yang, B.H. Loo, J. Electroanal. Chem. 443 (1998) 175–179.
[8] T. Maruyama, Y. Ikuta, J. Mater. Sci. 28 (1993) 5073–5078.
[9] D. Vernardou, M.E. Pemble, D.W. Sheel, Surf. Coat. Technol. 188–189 (2004) 250–254.
[10] M.N. Field, I.P. Parkin, J. Mater. Chem. 10 (2000) 1863–1866.
[11] M.G. Nolan, D.W. Sheel, M.E. Pemble, Electrochem. Soc. Pro. 2003–08 (2003) 417–423.
[12] H.M. Yates, M.G. Nolan, D.W. Sheel, M.E. Pemble, J. Photochem. Photobiol. A 179 (2006) 213–223.
[13] Y. Paz, Z. Luo, L. Rabenberg, A. Heller, J. Mater. Res. 10 (1995) 2842–2848.
[14] P. Sawunyama, L. Jiang, K. Hashimoto, J. Phys. Chem. B 101 (1997) 11000–11003.
[15] A. Mills, G. Hill, S. Bhopal, I.P. Parkin, S.A. O'Neill, J. Photochem. Photobiol. A 160 (2003) 185–194.
[16] M.C. Carotta, M. Ferroni, S. Gherardi, V. Guidi, C. Malagu, G. Martinelli, M. Sacerdoti, M.L.Di Vona, S. Licoccia, E. Traversa, J. Eur. Ceram. Soc. 24 (2004) 1409–1413.
[17] T.D. Manning, I.P. Parkin, Polyhedron 23 (2004) 3087–3095.
[18] U. Qureshi, T.D. Manning, I.P. Parkin, J. Mater. Chem. 14 (2004) 1190–1194.

[19] M.B. Sahana, M.S. Dharmaprakash, S.A. Shivashankar, J. Mater. Chem. 12 (2002) 333–338.
[20] X.Y. Li, X. Quan, C. Kutal, Scripta Mat. 50 (2004) 499–505.
[21] P. Prieto, R.E. Kirby, J. Vac. Sci. Technol. A13 (1995) 2819–2826.
[22] Y.J. Sun, T. Egawa, L.Y. Zhang, X. Yao Jpn. J. Appl. Phys. 41 (2002) L1389–L1392.
[23] J. Chastain, R.C. King, Handbook of X-ray Photoelectron Spectroscopy, Physical Electronic Inc., New York, 1995.
[24] G.W. Coulston, E.A. Thompson, N. Herron, J. Catal. 163 (1996) 122–129.
[25] S. Kaciulis, G. Mattogno, A. Napoli, E. Bemporad, F. Ferrari, A. Montenero, J. Elect. Spectroc. Rel. Phenom. 95 (1998) 61–69.
[26] D. Vernardou, Ph.D. Thesis, University of Salford, 2005.
[27] M. Nagashima, H. Wada, Thin Solid Films 312 (1998) 61–65.
[28] R. Gordon, J. Noncryst. Solids 218 (1997) 81–91.
[29] F. Beteille, R. Morineau, J. Livage, M. Nagano, Mater. Res. Bull. 32 (1997) 1109–1117.
[30] F.J. Morin, Phys. Rev. Lett. 3 (1959) 34–36.
[31] T.D. Manning, I.P. Parkin, R.J.H. Clark, D.W. Sheel, M.E. Pemble, D. Vernadou, J. Mater. Chem. 12 (2002) 2936–2939.
[32] Y. Muraoka, Z. Hiroi, Appl. Phys. Lett. 80 (2002) 583–585.
[33] J.L. Graham, C.B. Almquist, S. Kumar, S. Sidhu, Catal. Today 88 (2003) 73–82.
[34] H.J. Chae, I.-S. Nam, S.-W. Ham, S.B. Hong, Appl. Catal. B 53 (2004) 117–126.
[35] T. Garcia, B. Solsona, D.M. Murphy, K.L. Antcliff, S.H. Taylor, J. Catal. 229 (2005) 1–11.
[36] W. Choi, A. Termin, M.R. Hoffmann, J. Phys. Chem. 98 (1994) 13669–13679.
[37] A. Christodoulakis, M. Machli, A.A. Lemonidou, S. Boghosian, J. Catal. 222 (2004) 293–306.
[38] U. Qureshi, T.D. Manning, C. Blackman, I.P. Parkin, Polyhedron 25 (2006) 334–338.
[39] G. Zhao, H. Kozuka, H. Lin, T. Yoko, Thin Solid Films 329 (1999) 123–128.
[40] S. Klosek, D. Raffery, J. Phys. Chem. B 105 (2001) 2815–2819.
[41] J.C-S. Wu, C.H. Chen, J. Photochem. Photobiol. A 163 (2004) 509–515.
[42] E.P. Reddy, B. Sun, P.G. Smirniotis, J. Phys. Chem. B 108 (2004) 17198–17205.
[43] A. Fuerte, M.D. Hernandez-Alonso, A.J. Maira, A. Martinez-Arias, M. Fernandez-Garcia, J.C. Conesa, J. Soria, Chem. Commmun. (2001) 2718–2719.
[44] N.N. Greenwood, A. Earnshaw, Chemistry of the Elements, Pergamon Press, Oxford, 1984, pp.1144–1146.